JOURNAL OF AIRCRAFT
Vol. 44, No. 2, March–April 2007

Engineering Notes

ENGINEERING NOTES are short manuscripts describing new developments or important results of a preliminary nature. These Notes should not exceed 2500 words (where a figure or table counts as 200 words). Following informal review by the Editors, they may be published within a few months of the date of receipt. Style requirements are the same as for regular contributions (see inside back cover).

Wave Drag Characteristics of a Low-Drag Supersonic Formation Flying Concept

Yuichiro Goto,* Shigeru Obayashi,† and Yasuaki Kohama‡
Tohoku University, 2-1-1 Katahira Aoba-ku Sendai 980-8577, Japan

DOI: 10.2514/1.23236

Nomenclature

C_D	=	drag coefficient
C_L	=	lift coefficient
L/D	=	lift to drag ratio
M	=	freestream Mach number
r, θ, x_μ	=	three parameters for the skewed cylindrical coordinate system
x, y, z	=	three parameters for the cartesian coordinate system
x_w	=	streamwise coordinate along the wing surface
μ	=	Mach angle

I. Introduction

In the past 50 years, although the technology for transonic flight has matured, commercially practical civil supersonic transport has not been realized. The two major problems that have been preventing supersonic commercial transportation are wave drag and sonic boom.

Wave drag, which is the dominating component of drag at supersonic speeds, leads to a deterioration of cruise efficiency. And sonic booms have a problem of public acceptance, which imposes strict limitations on overland flights by supersonic transports. This leads to less flexible operation capabilities, reducing the profitability of their operation.

Many attempts have been made to minimize the wave drag and the sonic boom in the past. Among them, many studies approached this problem by optimizing the shape of the wing-body configuration. However, most studies have shown a strong tradeoff between wave drag and sonic boom, making it impossible to minimize wave drag and sonic boom simultaneously, for a given aircraft overall length.

The supersonic formation flying concept in this paper uses the benefits of multibody favorable wave interference to reduce the volume and lift dependent wave drag of the following aircraft. When aircraft fly through the air at supersonic speeds, they leave momentum in the air behind them, as shock waves and expansion fans. This is the cause of wave drag. This pressure gradient can be used to generate lift and thrust, which results in the collection of the momentum left in the air by the leading aircraft.

Friedman and Cohen [1] carried out linear analyses on bodies of revolution, imitating a fuselage and stores. As a result, they have shown that wave drag per total cross-sectional area can be reduced when placed in an optimal relative position. Positions of the stores that were favorable for wave drag reduction were positions where the stores were placed inside a shock wave, which is a positive pressure jump. The shock wave that impinges on the stores generate thrust, canceling a part of their drag.

In this paper, wave drag characteristics of this concept is investigated using Euler simulations. The dependence of wave drag to the relative position of the aircraft is investigated to evaluate the effectiveness of this concept and gain insight on the wave drag characteristics of supersonic formation flying.

II. Method

Euler simulations are carried out using TAS-flow, an unstructured Euler/Navier–Stokes solver, and the computational mesh was generated using EdgeEditor and TU TetraGrid, which are CFD tools developed at Tohoku University.

TAS-flow is an unstructured Euler/Navier–Stokes solver using a finite-volume cell-vertex scheme, HLLEW Riemann solver for flux computations [2], and LU-SGS implicit scheme for time integration [3]. EdgeEditor is an unstructured surface mesh generation software. It takes CAD data as an input [4], and generates a surface mesh using an advancing front triangulation method [5]. TU TetraGrid is an unstructured volume mesh generation software using the Delaunay triangulation algorithm [6].

As for the coordinate system used in this analysis, x is in the freestream direction, y is out towards the right wing tip, and z is upward. The origin of the coordinate system is located at the half-chord position along the centerline of the leading aircraft. x_w is used to express the streamwise position over the wing. $x_w = 0$ corresponds to the leading edge, and $x_w = 1$ corresponds to the trailing edge. The freestream Mach number used in this analysis is $M = 1.5$. This Mach number was chosen considering trends in the cruise Mach number of recent supersonic transport concepts.

Because the objective of this study is to investigate the effectiveness of supersonic formation flying, the subject of the analysis is kept simple to extract the effect of shock wave interaction alone, and facilitate the analysis. Therefore, in this paper, simulations are carried out on two aircraft formations. The model used for this study is an elliptical planform wing with a biconvex airfoil.

Although simplification of the configuration is convenient, the drag characteristics of the simplified model must be similar to that of a practical supersonic transport. The aspect ratio and thickness are determined so that the elliptical wing has a drag characteristic that is similar to a practical wing-body configuration [7]. A three-view diagram of this configuration is given in Fig. 1. This wing will be used as the aircraft in the formation.

In this paper, the angle of attack of the aircraft is fixed at $\alpha = 3.25$ deg. And the aerodynamic characteristics are evaluated by comparing the changes in both the C_L and C_D of the aircraft.

Presented as Paper 4604 at the AIAA 23rd Applied Aerodynamics Conference, Toronto, Canada, 6–9 June 2005; received 16 February 2006; revision received 17 July 2006; accepted for publication 29 July 2006.

*Graduate Student, Department of Aeronautics and Space Engineering. Student Member AIAA.
†Professor, Institute of Fluid Science. Associate Fellow AIAA.
‡Professor, Institute of Fluid Science.

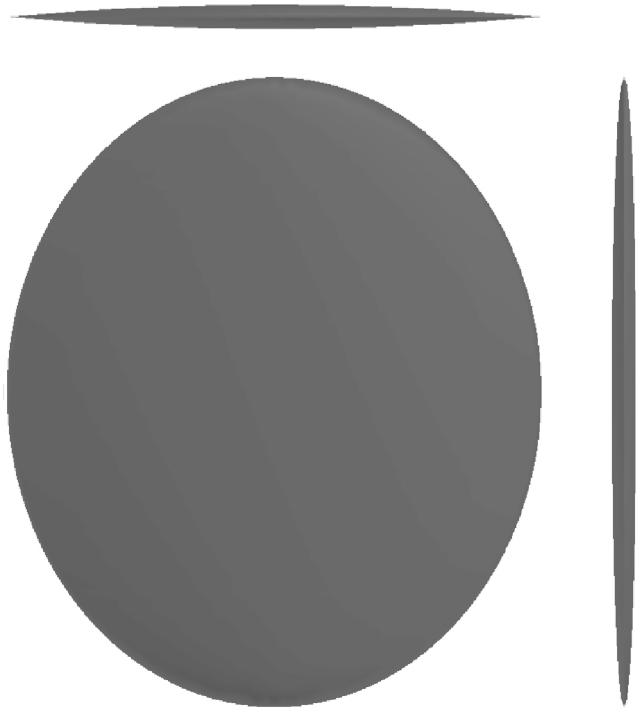

Fig. 1 Three-view diagram of the simplified aircraft.

The mesh used in this analysis is an unstructured full three-dimensional mesh with 1.05×10^6 grid points, and 42,000 grid points on each aircraft. The symmetry plane of this mesh is given in Fig. 2. A full three-dimensional mesh is used to allow for asymmetric formations. Grid convergence of the aerodynamic coefficients of the leading aircraft has been checked on several grids. The grid between the leading and trailing aircraft was fairly dense due to the fact that the region is in between two surfaces with dense surface mesh. This leads to a fairly clear shock wave with little dissipation. Adaptive grid refinement using pressure gradient as the sensor on several of the cases, but only less than 1% difference in C_L was observed. The refined grid size was approximately 3.5×10^6 grid points.

Aerodynamic coefficients were calculated from the flow simulation results on 63 different formations. The position of the following aircraft was chosen so that it is distributed over $y > 0$ half of the space behind the leading aircraft. Actual positions of following aircraft are shown in Fig. 3.

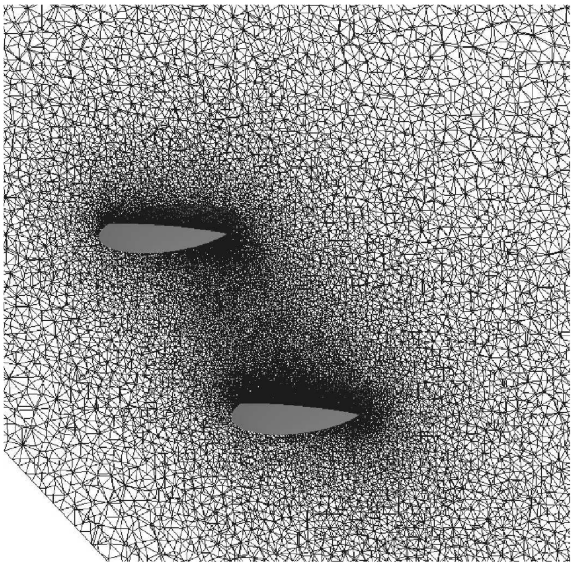

Fig. 2 Symmetry plane of computational mesh.

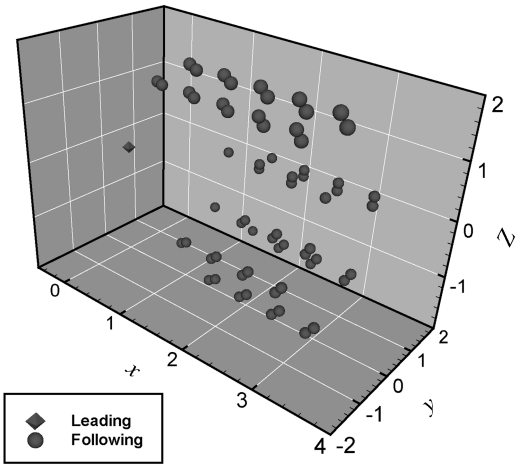

Fig. 3 Positions of the following aircraft in the investigated formations.

III. Results and Discussion

The values of the aerodynamic coefficients for the leading aircraft were $C_L = 0.1451$, $C_D = 0.01838$, and $L/D = 7.895$. These values were obtained by averaging the aerodynamic coefficients of the leading aircraft for the 63 formations, and will be used as the baseline condition, because the leading aircraft is flying in undisturbed freestream.

The best L/D of the following aircraft was achieved in Case 51. The following aircraft in this formation achieved a 17.9% improvement in L/D. The lift and drag coefficients of the following aircraft in this formation were $C_L = 0.12723$ and $C_D = 0.01367$. These values indicate that the improvement in L/D is achieved by reducing the drag. The C_p contour on the $y = 0$ plane is shown in Fig. 4. In this formation, the leading edge of the following aircraft is placed in the expansion fan of the leading aircraft.

To investigate the cause of this improvement in aerodynamic performance, the chordwise C_p distribution of the centerline of the aircraft are shown in Fig. 5. In this figure, the centerline C_p distribution of the following aircraft is plotted over that of the leading aircraft. Here, the reduction in C_p near the leading edge of the following aircraft is due to the impinging of the expansion fan extending from the leading aircraft. This resulted in the dramatic reduction in drag of the following aircraft. Near the midchord position of the following aircraft, there is a downward peak due to the

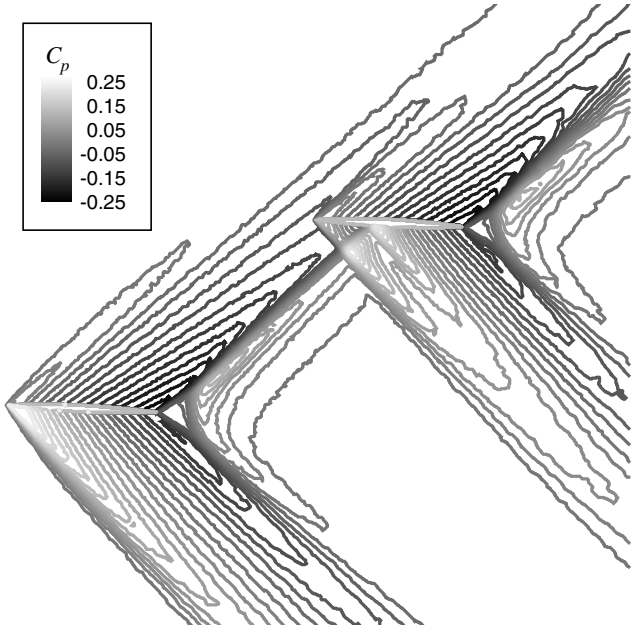

Fig. 4 C_p contour at $y = 0$, Case 51.

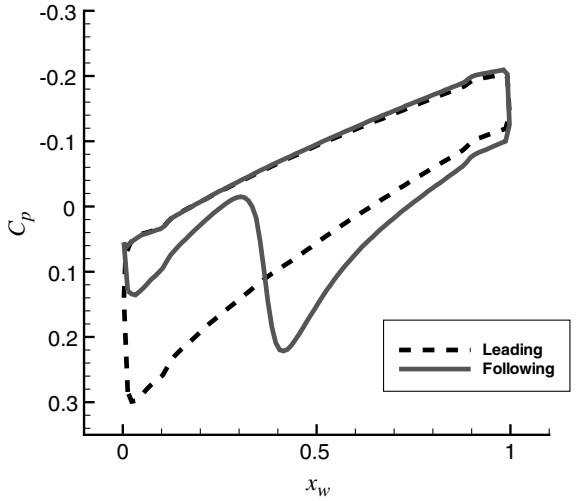

Fig. 5 Centerline C_p distributions of the leading and following aircraft, Case 51.

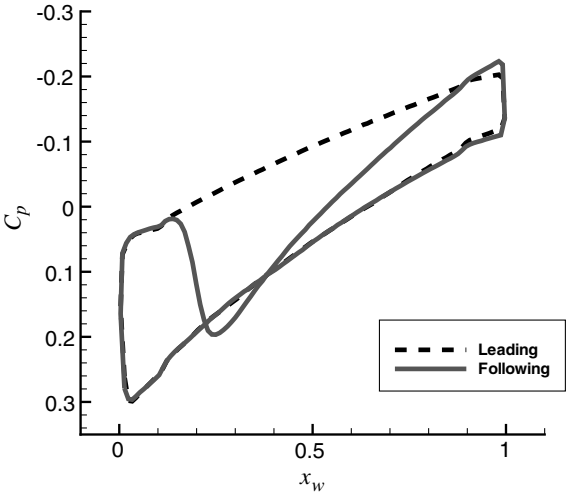

Fig. 7 Centerline C_p distributions of the leading and following aircraft, Case 1.

impinging of the shock wave extending from the trailing edge of the leading aircraft. This peak in C_p acts to compensate for the loss in lift caused by the impinging of the expansion fan.

On the other hand, the worst L/D was achieved in Case 1. The following aircraft, in this formation, experienced a 41.0% reduction in L/D. The lift and drag coefficients of the following aircraft were $C_L = 0.07111$ and $C_D = 0.01526$. Even though there was a considerable reduction in the drag of the following aircraft, this was not enough to compensate for the extensive reduction in lift. The C_p contour at the $y = 0$ plane is shown in Fig. 6. In this formation, the shock wave extending from the leading edge of the leading aircraft impinges on the upper surface of the following aircraft, leading to a reduction in lift.

To visualize the effect of the impinging shock wave more qualitatively, centerline C_p distributions are compared in Fig. 7. The C_p distribution of the following aircraft indicates that almost the whole upper surface of the following aircraft is being spoiled by the shock wave and the high pressure region extending from the leading aircraft, reducing the lift dramatically. But, the high pressure on the downstream half of the upper surface acts to reduce the wave drag exerted on the aircraft, although this benefit is not enough to compensate for the loss in lift.

To understand the dependence of wave drag on relative position more effectively, a new coordinate system, which takes into account the physics of the wave interaction, is introduced. In the new coordinate system, the position of the following aircraft is expressed using three parameters: r, θ, and x_μ. The conversion between the conventional Cartesian coordinate system and the new coordinate system is given by the following equations:

$$r = \sqrt{y^2 + z^2} \tag{1}$$

$$\theta = \arg(-z + yi) \tag{2}$$

$$x_\mu = x - r/\tan\mu \tag{3}$$

First of all, r is a parameter to express how far away along the Mach cone the following aircraft is located from the leading aircraft. To make the coordinate system intuitive, r is defined as the distance between the longitudinal axes of the leading and following aircraft. Next, θ is the azimuthal angle in the y–z plane. Here, θ is defined so that the following wing is placed below the leading aircraft when $\theta = 0$ deg, and the following wing is placed to the port side of the leading aircraft when $\theta = 90$ deg. And finally, x_μ expresses the streamwise position of the following aircraft with respect to the Mach cone extending downstream from the center of the leading aircraft. Although there are small discrepancies due to nonlinearity, x_μ can be regarded as a parameter that indicates how the following wing interacts with the shock waves and expansion fans. More specifically, if $x_\mu \approx -0.5$, then the upstream half of the following wing will be in undisturbed freestream and the leading-edge shock of the leading aircraft will be impinging near the midchord point of the following aircraft, and if $x_\mu \approx 0.0$, the leading edge shock of the leading aircraft will be impinging near the leading edge of the following aircraft, and so on.

Figure 8 is a diagram showing the relation between the conventional Cartesian coordinate system and the new coordinate system. In this figure, the conventional coordinate system is drawn in black dashed lines, the Mach cone is drawn in light gray lines, and the definition of the new coordinate system is drawn in black solid lines.

Aerodynamic performance of the 63 formations are analyzed using the new coordinate system.

First of all, aerodynamic performance values are compared against x_μ. Results are shown in Figs. 9–11. In these figures, different symbols correspond to subsets of data with different values of θ, and the aerodynamic performance of the leading aircraft is shown as a dashed line. Organized in the new coordinate system, the data points of most of the subsets of data form a fairly smooth single curve. This shows that the aerodynamic performance of the following aircraft shows good correlation with the parameter x_μ.

First, formations where $\theta = 0$ deg are investigated. In this case, the following aircraft is placed under the leading aircraft. Looking at

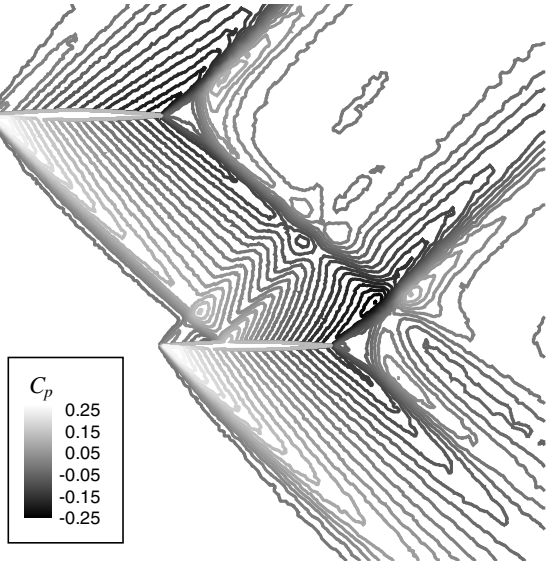

Fig. 6 C_p contour at $y = 0$, Case 1.

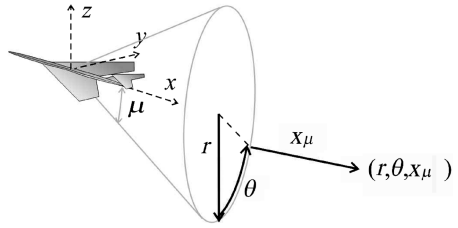

Fig. 8 Definition of the new coordinate system.

C_L, it has a peak near $x_\mu = 0.25$, and the performance deteriorates as values of x_μ get larger or smaller. This is due to the fact that the benefit of interaction with the expansion fan is greatest near this peak, and the effect of shock waves extending from leading and trailing edges of the leading aircraft take effect when x_μ moves off this value. Worst performance in C_L is seen near $x_\mu = -0.6$. This is due to the fact that if the following aircraft is placed too far forward, it stops interacting with the expansion fan, and stops receiving the benefits from the suction, while the impinging shock wave spoils its lift. C_D also has a maximum near $x_\mu = 0.0$. This is the position where the high pressure after the shock acts on the upstream half of the following aircraft, and the expansion fan impinges on the downstream half. Because the following aircraft exists inside this negative pressure gradient, the drag increases. When the following aircraft starts interacting with the leading-edge or the trailing-edge shock of the leading aircraft, it will be inside a positive pressure gradient, and this pressure gradient is used to generate lift and thrust. Looking at C_L, the most favorable position is near $x_\mu = 0.25$, and if C_D is considered, performance improves as x_μ moves away from 0.0. Therefore, as seen in Fig. 11, the best values for L/D exist near $x_\mu = 0.5$.

Next, formations where $\theta = 180$ deg are investigated. In this case, the following aircraft is placed above the leading aircraft. Here, C_L performance depicts an opposite trend compared to the previous case. The interaction with the shock waves, occurring at larger or smaller values of x_μ, maintains the value of C_L to be close to that of the leading aircraft, but interactions with the expansion fan reduces the C_L by about 40%. As for the value of C_D, lowest values of C_D are obtained when x_μ takes values near 0.5. Maximum value of L/D is obtained near $x_\mu = 0.70$.

Comparing the C_L and C_D for $\theta = 0$ and 180 deg, a difference can be seen in the occurring interaction. When $\theta = 0$ deg, drastic changes in these values are seen when x_μ takes small values, but when $\theta = 180$ deg, it is seen when x_μ takes medium to high values. This phenomenon can be understood if we take into account the lift dependent shock waves and expansion fans. When $\theta = 0$ deg, the leading-edge shock wave is stronger compared to the expansion fan downstream, resulting in a strong effect on aircraft flying at small values of x_μ. On the other hand, when $\theta = 180$ deg, the expansion fan is stronger and strongly affects aircraft flying at medium to high values of x_μ.

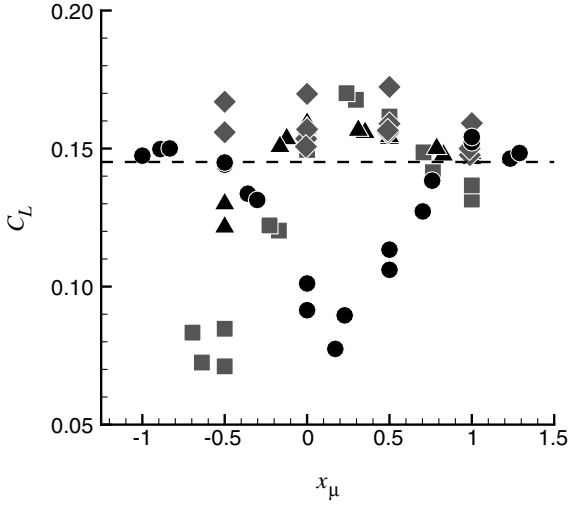

Fig. 9 C_L for all formations plotted to x_μ.

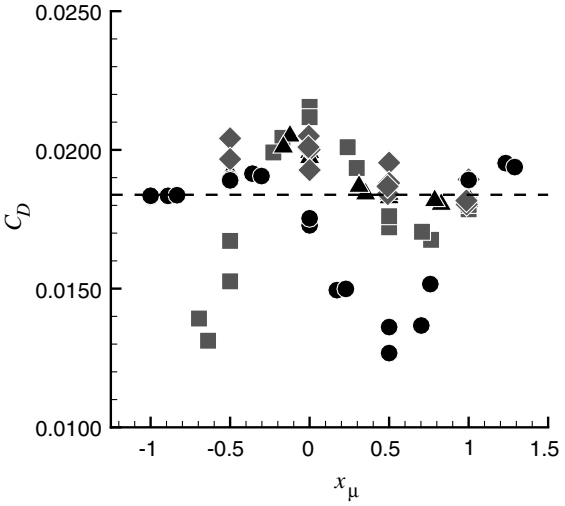

Fig. 10 C_D for all formations plotted to x_μ.

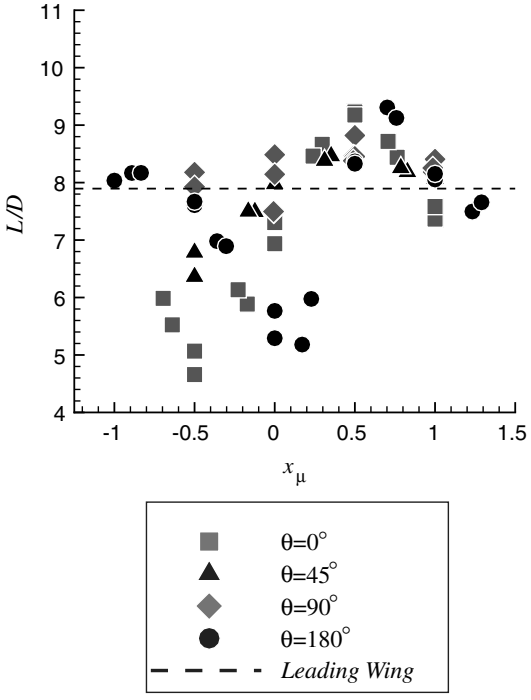

Fig. 11 L/D for all formations plotted to x_μ.

In these two cases, the sensitivity of aerodynamic performance to x_μ is evaluated. Looking at the C_L and C_D plots in the region where the formations achieved best L/D, in both cases, the C_L and C_D plots have a very steep slope. This is indicating that these aerodynamic coefficients are changing drastically in this region. This drastic change in aerodynamic performance may cause stability and control problems when in actual flight. Position keeping in cruise may need active automatic controlling, and also, transitioning into this formation may be even more difficult.

In cases where $\theta = 45$ and 90 deg, improvement and deterioration from the performance of the leading aircraft is smaller than in previous cases. Looking at the C_p contour plots of the flowfield behind the leading aircraft, shock waves and expansion fans propagating in the vertical direction were stronger than those propagating in the horizontal direction. Therefore, more momentum propagates in the vertical plane, and the amount of momentum in the

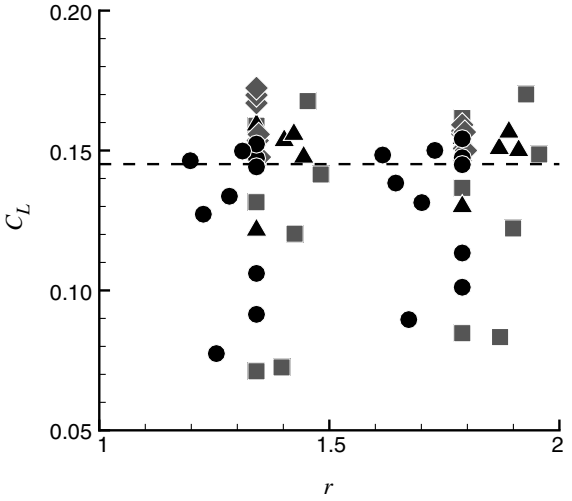

Fig. 12 C_L for all formations plotted to r.

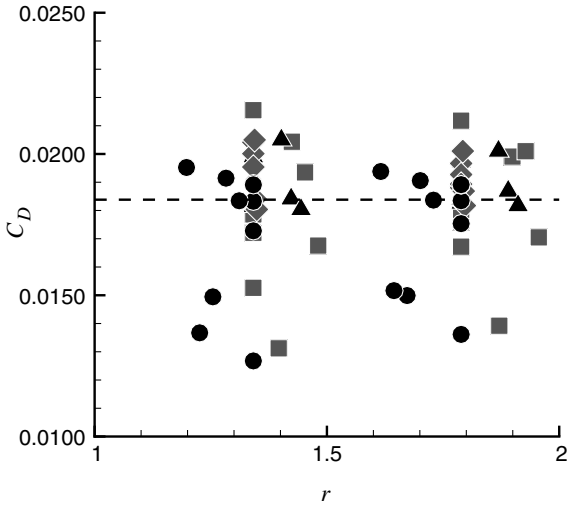

Fig. 13 C_D for all formations plotted to r.

air that the following aircraft can recover from the flowfield becomes less as the following aircraft moves off the $y = 0$ plane. But, on the other hand, aircraft handling characteristics for the following aircraft will improve, as the effect of wave interaction becomes moderate.

Next, aerodynamic performance is plotted against r in Figs. 12–14 to investigate the dependence on the distance between the two aircraft. Here, it can be seen that, as the distance between the two aircraft increase, the data points move closer towards the values of the leading aircraft. This indicates that the effect of wave interaction becomes weaker as the distance between the aircraft increase. This reduces the benefits of wave interaction, but on the other hand, may result in more moderate dynamic characteristics.

IV. Conclusions

In this study, the drag characteristics of a concept to achieve low drag by formation flying of supersonic transports has been investigated. The drag characteristics have been checked for different arrangements of the formation. From these results, it can be concluded that the supersonic formation flying concept showed up to 17.9% increase in L/D and therefore deserves further research as a means to reduce the wave drag of a fleet of supersonic aircraft. The best L/D values were achieved when the following aircraft interacts with the expansion fan of the leading aircraft.

To organize the data taking into account the physics of the drag reduction mechanism, a new coordinate system, which is made up of parameters that indicate the degree of interaction with the shock and expansion fans, has been introduced. This coordinate system has been proven to be very effective in categorizing the patterns of wave interference. In this coordinate system, the interaction with shock and expansion fans is dominated by x_μ, and the effect of diffusion of the shock and expansion fans is expressed by r. This coordinate system also succeeded in showing the sensitivity of wave drag to the relative position of the aircraft. Results indicated that different formations have different degrees of sensitivity, and θ could be adjusted to trade off performance for dynamic characteristics.

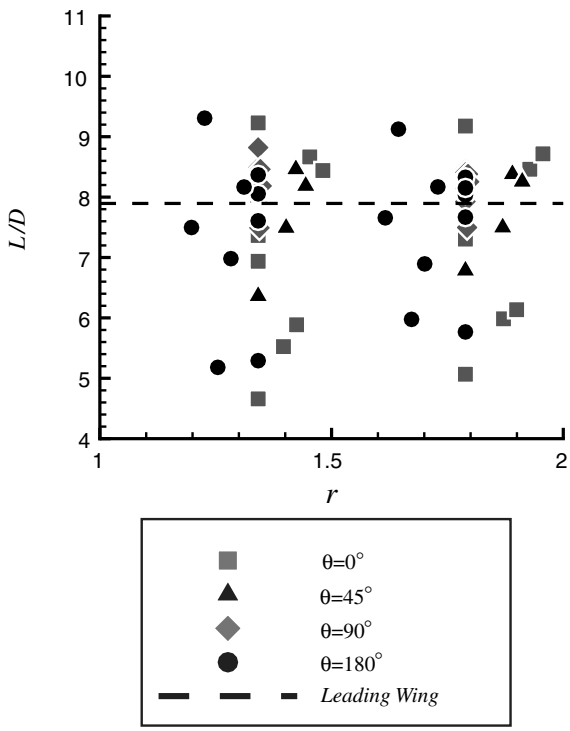

Fig. 14 L/D for all formations plotted to r.

Acknowledgments

This work was supported by a 21st Century COE Program Grant of the International COE of Flow Dynamics from Ministry of Education, Culture, Sports, Science and Technology. Authors would also like to thank K. Nakahashi and the Spacecraft Systems Laboratory, Department of Aerospace Engineering, Tohoku University for providing the CFD analysis tools.

References

[1] Friedman, M. D., and Cohen, D., "Arrangement of Fusiform Bodies to Reduce the Wave Drag at Supersonic Speeds," NACA Report 1236, 1955.

[2] Obayashi, S., and Guruswamy, G. P., "Convergence Acceleration of an Aeroelastic Navier-Stokes Solver," *AIAA Journal*, Vol. 33, No. 6, 1994, pp. 1134–1141.

[3] Sharov, D., and Nakahashi, K., "Reordering of Hybrid Unstructured Grids for Lower-Upper Symmetric Gauss-Seidel Computations," *AIAA Journal*, Vol. 36, No. 3, 1998, pp. 484–486.

[4] Ito, Y., and Nakahashi, K., "Surface Triangulation for Polygonal Models Based on CAD Data," *International Journal for Numerical Methods in Fluids*, Vol. 39, No. 1, 2002, pp. 75–96.

[5] Ito, Y., and Nakahashi, K., "Direct Surface Triangulation Using Stereolithography Data," *AIAA Journal*, Vol. 40, No. 3, 2002, pp. 490–496.

[6] Sharov, D., and Nakahashi, K., "A Boundary Recovery Algorithm for Delaunay Tetrahedral Meshing," *Proceedings of the 5th International Conference on Numerical Grid Generation in Computational Field Simulations*, 1996, pp. 229–238.

[7] Goto, Y., Obayashi, S., and Kohama, Y., "Drag Characteristics of a Low-Drag Low-Boom Supersonic Formation Flying Concept," AIAA Paper 2005-4604, 2005.